
Article:
Mitra, B., Hilden, J. and Litster, J. orcid.org/0000-0003-4614-3501 (2018) Assessment of intragranular and extragranular fracture in the development of tablet tensile strength. Journal of Pharmaceutical Sciences, 107 (10). pp. 2581-2591. ISSN 0022-3549

https://doi.org/10.1016/j.xphs.2018.05.011

Assessment of intra-granular and extra-granular fracture in the development of tablet tensile strength

Biplob Mitra[1,2,3], Jon Hilden[2,4], James D Litster[5,6]

[1]Drug Product Development, Celgene Corporation, Summit, NJ, USA

[2]Small Molecule Design and Development, Eli Lilly and Co., Indianapolis, IN, USA

[3]Department of Industrial and Physical Pharmacy, Purdue University, West Lafayette, IN, USA

[4]School of Materials Engineering, Purdue University, West Lafayette, IN, USA

[5]Department of Chemical and Biological Engineering, University of Sheffield, Sheffield, UK

[6]School of Chemical Engineering, Purdue University, West Lafayette, IN, USA

ABSTRACT:

When a tablet is compacted from deformable granules and then broken, the fracture plane may cleave granules in two (intra-granular fracture) or separate neighboring granules (extra-granular fracture). In this study, a novel method was developed to quantify the extent of intra- versus extra-granular fracture by compacting tablets from multi-colored ideal granules and evaluating fracture surfaces. The proportions of intra-granular and extra-granular fracture were quantified and modeled in light of a new metric, the deformation potential, Δ, reflecting the solid fraction increase as an initial granule bed is compressed into a final tablet. Results show that a measurable tablet strength is achieved at $\Delta > 0.18$, but intra-granular fracture is not observed until $\Delta > 0.21$. At very large Δ, tablets experience almost exclusively intra-granular fracture, yet the tablet tensile strength is considerably lower than that of a tablet compacted from raw powders versus pre-compacted granules. Thus, secondary compaction of granules appears to weaken the granule matrix, leading to reduced tablet tensile strength even in the presence of strong extra-granular bonding.

KEYWORDS: Tablet, Granulation, Compaction, Mechanical Properties, Solid Fraction, Deformation Potential, Tensile Strength, Image Analysis, Intra-granular Fracture, Intra-granular Strength

Correspondence to:
Biplob Mitra, PhD, RPh
Drug Product Development
Celgene Corporation
181 Passaic Avenue
Summit, NJ 07901, USA
bmitra@celgene.com, bkmitra@yahoo.com

1. Introduction

Pharmaceutical tablets can experience a range of mechanical stressors from multiple sources including the tumbling action inside a tablet coating pan, vibration and impact during bulk transport in bottles, or from being forcefully pushed through the foil backing of a blister pack. In these cases, it is desirable to avoid tablet fracture. Fracture not only affects tablet elegance, but can also increase the risk of unintended exposure to care givers in cases where the tablet coating helps contain the medicine within. A mechanistic understanding of tablet fracture is therefore highly desirable.

The transformation of powder into a coherent tablet structure is essentially an inter-particle bonding process. However, the majority of pharmaceutical powders fed to a tablet press are not primary particles, but granular, porous secondary particles. Powders are often converted into granules via various granulation techniques and then forward processed into tablets to achieve desired quality attributes of the final product (such as mechanical strength, content uniformity, dissolution) and/or to improve process performance. Tablets prepared from granules can be described as granules bonded together. In addition to the mechanical properties of the primary particles and granules, the physical changes that occur to granules during the confined compression process are also important in evolution of the tablet structure. In the development of a quality tablet dosage form, a balance between physical (e.g., appearance) and mechanical (e.g., solid fraction (SF), tensile strength (TS)) properties of tablets and their performance (e.g.,

disintegration time, dissolution) must be maintained. Use of mechanistic understanding in selecting material attributes and/or process parameters to design a tablet product can potentially ensure robustness of the product quality attributes.

To mechanistically explain the strength of tablets formed from granules, the process of fracture has attracted considerable interest. The TS of pharmaceutical tablets has been explained in view of the phenomena that generally occur in metal (Hall-Petch relationship [1, 2]) and ceramic compacts (Griffith's crack criterion [3, 4, 5]). In fact, Sun et al. [6] and others [7, 8, 9] have used milled granules of microcrystalline cellulose (MCC) and showed that larger granule sizes lead to lower tablet TS. Relationships between TS, critical stress intensity and crack size have also been reported in literature [10, 11, 12]. However, mechanical properties of pharmaceutical materials such as ductility and brittleness are generally ranked between metal and ceramic materials. It is not clear whether the Hall-Petch relationship nor fracture mechanics can be applied to pharmaceutical materials such as MCC. Dislocation glide is not the expected deformation mechanism in MCC. Fracture of an MCC tablet by crack propagation is also less likely to occur because of the potential blunting of the crack-tip by plastic deformation [13]. Moreover, the crack length is a critical parameter that cannot be easily determined [14]. The largest crack is not necessarily located on the fracture plane.

TS of tablets have also been modeled using the bond summation concept which is based on Rumpf's theory of strength of agglomerates [15]. TS of a tablet is governed by the inter-particular bonding force and the bonding area in a given cross section that fails under an applied stress [16, 17]. Johansson et al. [18] showed that low and high SF MCC pellets achieved larger and smaller bonding area in the tablet, respectively. For the bond summation concept to work, it is critical to determine the actual bonding surface area and the bonding force. However, it is difficult to quantify the directly.

In the literature [18, 19, 20, 21], there is a common perception that the fracture plane of tablets prepared from granules is created between the neighboring granules. In contrast, our previous study [22] demonstrated that high SF tablets prepared from low SF granules fracture indiscriminately both intra- and extra-granularly and produce a smooth fracture plane.

Conversely, low SF tablets prepared from high SF granules fracture extra-granularly by separating neighboring granules. A common perception also exists that intra-granular bonding strength is higher than extra-granular bonding strength in a tablet [18, 21].

In this work a mechanistic model of tablet compression and strength evolution is proposed and explored experimentally by examining the fracture planes on matching halves of broken tablets prepared from novel, multi-colored monodisperse granules. The model explores basic phenomena that transpire as a bed of porous granules is compressed into a tablet and then broken. This includes the densification of individual granules with increasing compaction stress and associated evolution of granule strength as well as the formation of bonds between granules and the associated evolution of extra-granular bond strength. The novel use of multi-colored monodisperse granules in this work permits the experimental quantification of intra-granular fracture versus extra-granular fracture when compacted tablets are broken. These fracture areas are examined under different conditions of initial granule solid fraction and final tablet solid fraction. Analysis of these results leads to the identification of a new variable, the deformation potential, as being critical to the formation of extra-granular bonds and the evolution of tablet strength. Results also suggest that the inherent weakening of granules due to repeated deformation (first in the granulation process and then again in the tablet compaction process) is the dominant factor leading to decreased tablet TS.

2. Mechanistic Model to Predict Tablet Tensile Strength

The fracture of tablets composed of compressed granules can occur along two possible paths. The first occurs when the fracture plane propagates along the shortest possible path, cleaving granules and serving to minimize the fracture surface area regardless of the relative position of grain boundaries. This is expected when the strength of the grain boundaries (i.e. the extra-granular bond strength), σ_{EG}, is the same or higher than the strength of the granule matrix (i.e. the intra-granular bond strength), σ_{IG}. The resulting fracture surfaces are flat and smooth with minimum surface area. The second occurs when the fracture plane propagates entirely between the granules, separating neighboring granules as it passes. This is expected when the grain boundaries are weak compared to the granule strength (i.e. $\sigma_{IG} > \sigma_{EG}$). The resulting fracture

surfaces are rough and exhibit topography associated with the size and shape of the freshly separated granules.

The most general, and perhaps the most common case is a combination. The fracture plane cleaves some granules but also separates granules when convenient (e.g. when grain boundaries are close by and moderately parallel to the fracture plane). For the general case, the overall tablet strength, σ_T, can be modeled as a combination of both fracture paths:

$$\sigma_T = A_{IG} \cdot \sigma_{IG} + A_{EG} \cdot \sigma_{EG} \quad (1)$$

where A_{IG} and A_{EG} are the area fractions of intra- and extra-granular fracture, respectively. While σ_T can be measured easily using a diametrical compression test, other approaches are needed to either predict or measure the variables on the right hand side of eqn.1. These approaches are discussed below.

2.1. Estimation of A_{IG} and A_{EG}

Analytical methodologies were developed and experiments were performed in this work to quantify the extent of intra-granular versus extra-granular fracture during diametrical compression testing (aka "hardness" testing) of round tablets. The approach was developed based on the pictorial model described in Figure 1. Tablets were prepared from mixtures of equal numbers of monodisperse granules of four different colors (white, blue, red and grey). Fracture by the diametrical compression test produced two fracture surfaces of tablets. If the granule color was different on each side of the fracture plane then fracture occurred extra-granularly (i.e. along grain boundaries). If the granule color was the same on each side, then either fracture occurred intra-granularly, or it occurred extra-granularly between two neighboring granules of the same color.

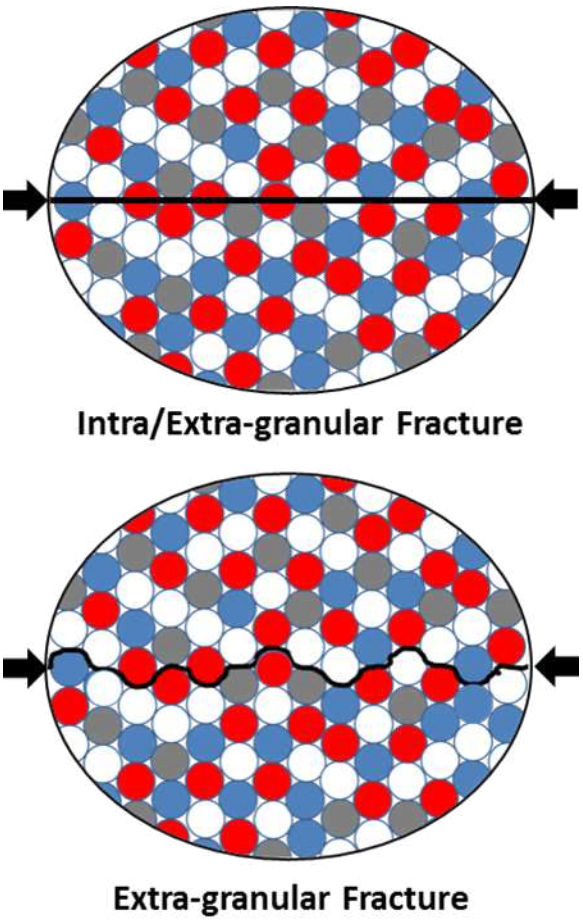

Figure 1. Illustration of the Approach to Quantify Intra-granular and Extra-granular Fracture of Tablets.

On average, the probability of two neighboring granules having the same color is 25% because of the equal mixing proportions of four colors of granules. Thus, we can write:

$$A_m = A_{IG} + \frac{1}{4} \cdot A_{EG} \tag{2}$$

where A_m denotes the area fraction where colors match on both sides of the fracture surface. Noting that the area fractions of matched colors and fracture types must both sum to unity provides:

$$A_m + A_{mm} = 1 \tag{3}$$

$$A_{IG} + A_{EG} = 1 \tag{4}$$

where A_{mm} denotes the area fraction where colors are mis-matched on both sides of the fracture surface. Combining equations 2-4, one can determine the intra-granular and extra-granular fracture area fractions as:

$$A_{IG} = \frac{1}{3}(4A_m - 1) \tag{5}$$

$$A_{EG} = \frac{4}{3} \cdot A_{mm} = \frac{4}{3}(1 - A_m) \tag{6}$$

2.2. Prediction of σ_{IG}

The prediction of granule tensile strength, σ_{IG}, for use in Equation 1 requires two steps. First, σ_{IG} must be established as a function of granule solid fraction, SF_G. Second, SF_G must be estimated as a function of the overall tablet solid fraction, SF_T, since it is not possible to measure the solid fraction of granules directly within a tablet.

The relation between σ_{IG} and SF_G can be measured directly on granules without including them in a tablet by making granules at different solid fractions and measuring their tensile strength by diametrical compression. The resulting data set can be fit to an exponential equation as follows:

$$\sigma_{IG} = c \cdot exp(d \cdot SF_G) \tag{7}$$

where, c and d are material-dependent coefficients. Values of c and d can be established by regressing $\mathrm{Ln}(\sigma_{IG})$ against SF_G. Equation 7 can thus be used to predict σ_{IG} if SF_G is known.

Unfortunately, while it is easy to measure the initial granule solid fraction, SF_G^i, as well as the final tablet solid fraction, SF_T, it is not practical to measure the final solid fraction of granules within the tablet, SF_G^f. Thus an additional equation must be established to estimate SF_G^f as a function of SF_T and SF_G^i. The requirements of the equation are that:

1) The curve must pass through the initial condition where both SF_G^i and SF_T are known.
2) SF_G^f must be greater than SF_T at all values of SF_T since the packing fraction is always <1.
3) SF_G^f increases monotonically with SF_T.
4) SF_G^f approaches 1 as SF_T approaches 1.

5) The slope dSF_G^f/dSF_T approaches 1 as SF_T approaches 1.

We find the following exponential equation to be useful in meeting these requirements:

$$SF_G^f = -\frac{e^{p\cdot(1-SF_T)}}{p} + \left(1+\frac{1}{p}\right) \tag{8}$$

where, p is a fitting parameter adjusted to meet the initial condition (requirement 1).

2.3. Deformation Potential

As described above, tablet tensile strength is affected by both the initial granule solid fraction, SF_G^i, and (final) tablet solid fraction, SF_T. In this work we combine these variables to provide a revised [22] definition of the deformation potential, Δ. The deformation potential is defined as the difference between the final SF of the compacted tablet and the initial solid fraction of the un-compacted bed of granules, SF_{bed}. Δ and SF_{bed} are thus defined as:

$$\Delta = SF_T - SF_{bed} \tag{9}$$

and

$$SF_{bed} = (1-\varepsilon_b)SF_G^i \tag{10}$$

where ε_b denotes the voidage of the packed bed. The voidage is defined as the space between granules and is a function of granule shape and packing, but not of granule solid fraction. The packed bed can thus be considered as a "tablet" with zero strength. As the bed is compacted into a tablet (Figure 2), the granules will deform plastically. Deformation will occur by both densification of granules and by the plastic "flow" of granules into available void space. Both mechanisms lead to increased tablet solid fraction and strength. Combining Equations 9 and 10 yields:

$$\Delta = SF_T - (1-\varepsilon_b)SF_g^i \tag{11}$$

Thus Δ=0 for an un-compacted bed of granules and Δ increases with increasing SF_T or with decreasing SF_g^i. Consequently, tablet strength is expected to increase with increasing Δ and

fracture of a tablet with low Δ is expected to occur by separation of granules with little or no intra-granular fracture.

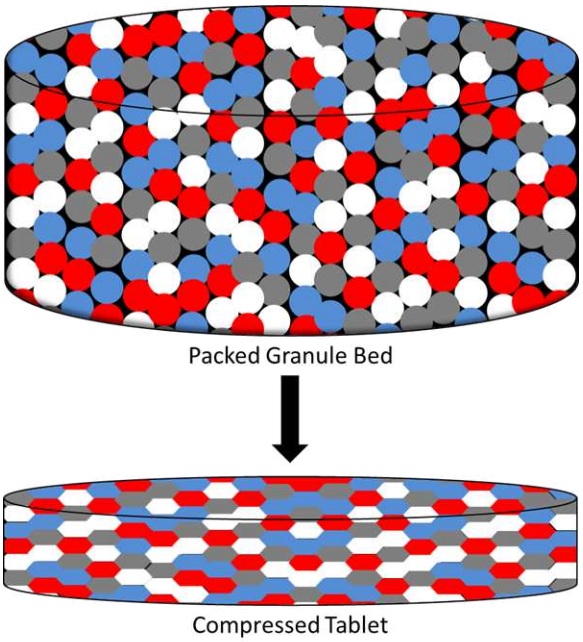

Figure 2. Illustration of Deformation of Granules During Compression.

3. Materials and Methods

3.1. Virgin Microcrystalline Cellulose (V-MCC)

In this study, microcrystalline cellulose (Avicel PH200, FMC, PA, USA) was used as the starting material to produce monodisperse granules, which were forward processed into tablets. Figure 3 illustrates the schematic diagram of the study design.

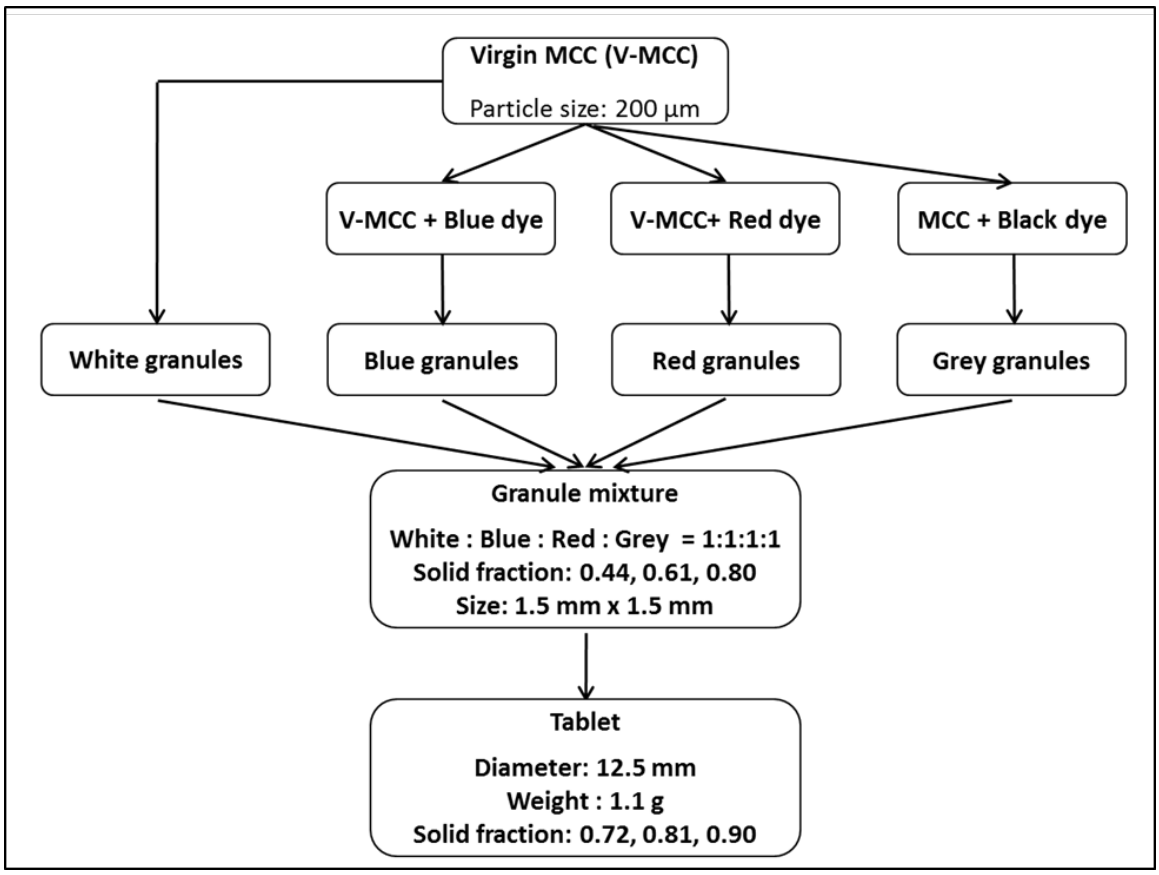

Figure 3. Schematic Diagram of the Study Design.

A sieve fraction of 150-250 µm of MCC powder was obtained using a rotary sieve apparatus (Rotap RX29), and was referred to as 200 µm V-MCC. V-MCC was equilibrated at 20°C/30% RH condition for 24 hours prior to forward processing to eliminate the impact of moisture content variability on the compact's mechanical properties [23]. The apparent density of V-MCC powder was determined to be 1.556 g/cc by helium pycnometry which was consistent with the literature [24].

3.2. Monodisperse Granule Preparation

V-MCC was mixed with 2% (w/w) FDC blue 2, iron oxide red or iron oxide black powder using a Turbula mixer (model T2F, Willy A. Bachofen AG, Basel, Switzerland) for 10 minutes at 32 rpm to obtain blue, red or grey colored MCC powders, respectively. White, blue, red and grey colored monodisperse granules of precisely controlled size (1.5 mm diameter x 1.5 mm thickness), shape (biconvex cylindrical compact), and SF (nominally 0.44, 0.61 and 0.80) were

produced by directly compressing V-MCC and colored MCC powders. A Korsch EK0 (Korsch Pressen, Berlin, Germany) tablet press equipped with standard concave, multi-tip tooling was used. SF of granules were controlled by varying the granule weight while keeping the granule thickness the same. The press speed was 30 strokes/ min. To condition for moisture content and allow post ejection relaxation, monodisperse granules were equilibrated at 20°C/30% RH for 24 hours and stored in airtight glass containers until being characterized (for weight, thickness, and breaking force) and forward processed into tablets. Neither the V-MCC powder nor the monodisperse granules were lubricated in this study.

3.3. Compression of Tablets from Colored Monodisperse Granules

A list of tablets prepared from monodisperse granules is shown in Table 1. At each granule SF, equal proportions of granules, by weight, of all four colors were mixed together for 10 minutes at 32 rpm on a Turbula mixer (model T2F, Willy A. Bachofen AG, Basel, Switzerland) prior to compaction. For each set of conditions, five tablets (n=5), weighing 1.1 g each were made using an Instron universal testing machine (model 5569, Instron Ltd. Buckinghamshire, United Kingdom) equipped with 12.5 mm flat face tooling. The compression and decompression rate was 50 mm/min with zero dwell time. The die wall was lubricated with magnesium stearate powder. Compressive stresses of approximately 60, 100 and 200 MPa were used to produce tablets with nominal SF of 0.72, 0.81, and 0.90. To allow post ejection relaxation, tablets were stored in airtight scintillation glass jars for at least 24 hours prior to measuring weight, thickness, and breaking force.

Table 1. Colored Granule Mixtures and Tablets Prepared There From

V-MCC Particle Size (μm)	Colored Granule Mixtures				Tablet Solid Fraction
	Diameter (mm)	Nominal Thickness (mm)	Nominal Volume (mm^3)	Nominal Solid Fraction	
200	1.5	1.5	2.0	0.44 0.61 0.80	0.72 0.81 0.90

3.4. Physical Characterization of Granules and Tablets

The apparent density of colored V-MCC was determined from the weight fractions and apparent densities of individual constituents [25]:

$$\rho_{mix} = \frac{m_1+m_2}{\frac{m_1}{\rho_1}+\frac{m_2}{\rho_2}} \quad (12)$$

where m and ρ denote the weight percent and apparent density of constituent powder, respectively.

Monodisperse granules and tablets were characterized out-of-die for weight, thickness, and breaking force at least 24 hours after compression. Solid fractions were calculated as [25].

$$SF = \frac{(m/\rho_{mix})}{2 \cdot V_{cup} + A_{die}\ (t - 2 \cdot d_{cup})} \quad (13)$$

where m, ρ_{mix}, V_{cup}, A_{die}, t and d_{cup} are defined as compact mass, apparent density of powder mix, cup volume of the punch, die hole area, out-of-die thickness of the compact, and cup depth of the punch, respectively. Tapped SF of the granule bed was determined from the tapped density and the initial granule SF using eq. 10 and the deformation potential using eq. 11.

The breaking force of monodisperse granules was measured using a Zwick Testing System (Zwickiline 2.5kN, Zwick GmbH & Co. Germany) equipped with a Zwick Xforce 500 N load cell and 10 mm compression platens. Breaking forces of tablets were measured using an Instron universal testing machine (model 5569, Instron Ltd. Buckinghamshire, UK) equipped with a 1 kN load cell and 50 mm diameter upper and lower platens. The upper platen compression rate was 10 mm/min for both equipment. Out-of-die thicknesses of compacts were measured using a Mitutoyo Absolute digital thickness gauge (Mitutoyo Mexicana S.A., Mexico). Weights of monodisperse granules and tablets were measured using a Mettler Toledo AE240 or Mettler Toledo XP56 balance (Mettler-Toledo, OH, USA).

Tensile strengths of monodisperse granules (biconvex cylindrical compacts) and flat-faced round tablets were calculated using the following relation [22, 26]:

$$TS = \frac{F_c \cdot D}{2 \cdot V_{eq}} \quad (14)$$

where F_c, D, and V_{eq} are defined as diametrical breaking force of the compact, diameter of the compact, and volume of the compact, respectively. Recent work suggests that tensile strengths calculated with this equation are likely in error by a factor of two [27]. However, the relation is used here for consistency with other works.

The volume of monodisperse granules was calculated as:

$$V_{eq} = \frac{\pi \cdot D^2 \cdot (t - d_{cup})}{4} + 2 \cdot V_{cup} \quad (15)$$

where D, t, d_{cup} and V_{cup} are defined as diameter of the compact, total thickness (out-of-die) of the compact, cup depth of the tooling and cup volume of the tooling, respectively.

3.5. Mapping of the Fracture Surfaces of Tablets for Intra-granular and Extra-granular Fracture

Optical images of monodisperse granules, tablets and fracture surfaces of tablets were taken using a Keyence digital microscope (VHX 2000, Keyence America, IL, USA). The area of differing color between the two fracture surfaces of a tablet was initially measured using a macro developed in the FIJI distribution of ImageJ software [28, 29, 30, 31]. However, the automated process was found to be extremely sensitive to subtle changes in lighting and after several attempts was deemed unreliable for quantitative analysis. As a result, a manual method was also developed in which a grid was overlaid on each fracture surface as shown in Figure 4 and aligned with position/orientation of each mating fracture surface. The grid contained 275 intersections. The intersections with same alphanumerical identities are the adjacent points on the two fracture surfaces; the two corresponding points were circled if their colors did not match as shown in Figure 4. The area fraction of mismatched colors, A_{mm}, (e.g. for use in Equation 6) was estimated as the number of circles divided by the total number of intersections.

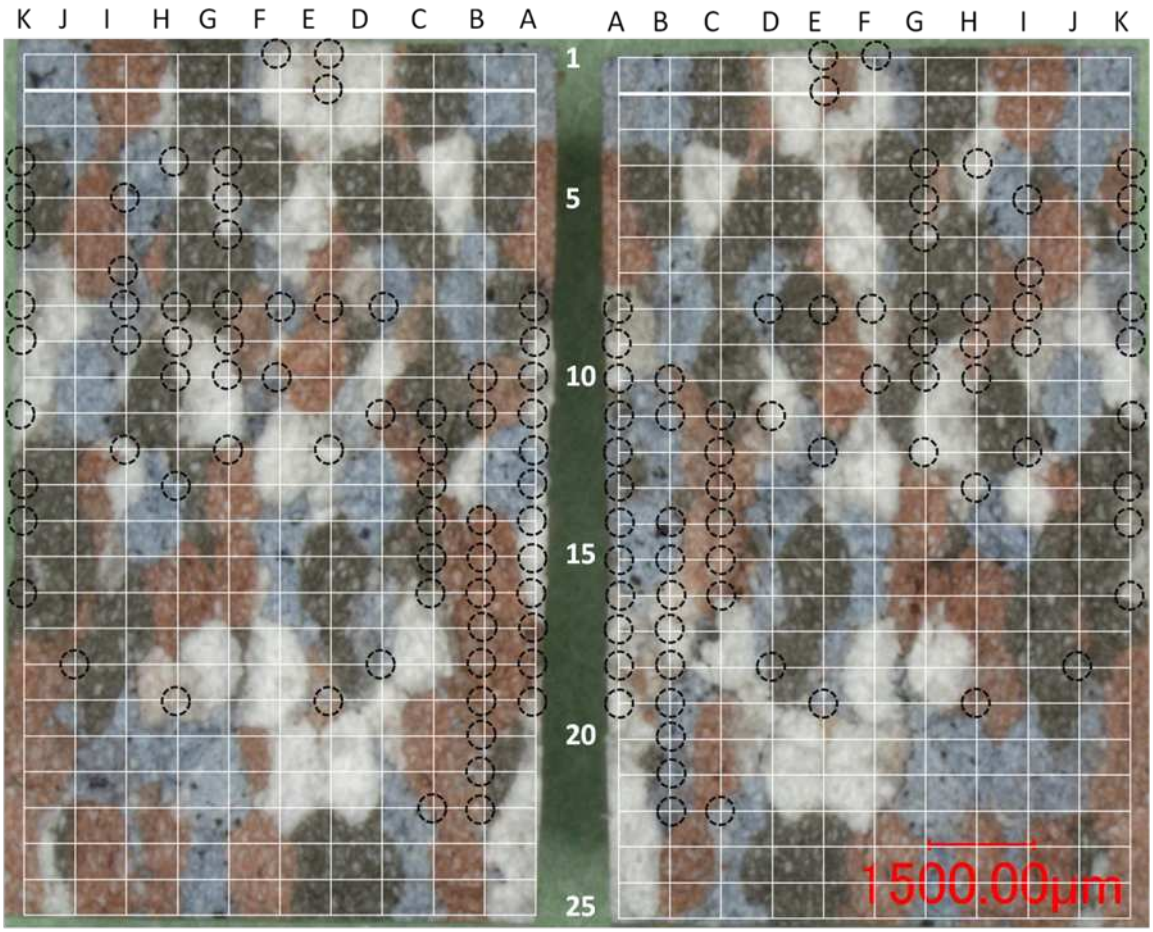

Figure 4. Image Analysis Using a Grid Overlay.

4. Results

4.1. Granule Characterization

Granule tensile strengths are plotted as a function of granule solid fraction in Figure 5. The data show that granule TS increases approximately exponentially with increasing granule SF, which is consistent with literature [32]. An exponential regression was performed (R^2=0.98) resulting in regression constants of $\boldsymbol{c = 0.0292}$ and $\boldsymbol{d = 6.7922}$ for use in Equation 7. During testing, granules were observed to fracture along the centerline, indicative of tensile failure, and the calculated tensile strength was found to be unaffected by granule color.

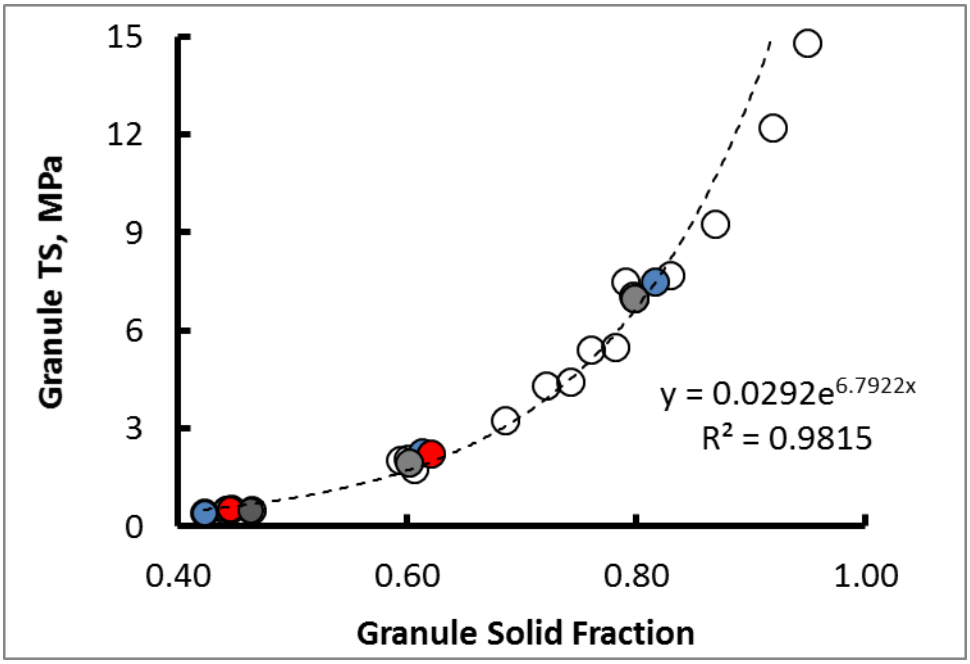

Figure 5. Tensile Strength of Granules Versus Granule Solid Fraction.

4.2. Deformation Potential

Granule bed packing fractions ($1 - \varepsilon_b$) and solid fractions (SF_{bed}) of tapped cylindrical beds of granule mixtures are summarized in Table 2 along with final tablet solid fractions and associated deformation potentials. For all three sets of granules, the packing fraction was slightly lower than the packing fraction (0.64) of randomly packed monodisperse spheres as reported in literature [33]. SF_{bed} increased as the initial SF of granules SF_G^i increased. At a given tablet SF, the deformation potential (Δ) is higher for low SF granules than for high SF granules.

Table 2. Properties of Packed Granule Bed Prior to Compaction

Initial Granule Solid Fraction (SF_G^i)	Packed Granule Bed		Tablet Solid Fraction (SF_T)	Deformation Potential (Δ)
	Packing Fraction ($1-\varepsilon_b$)	Solid Fraction (SF_{bed})		
0.44	0.58	0.26	0.72 0.81 0.90	0.46 0.55 0.64
0.61	0.58	0.35		0.37 0.46 0.55
0.80	0.61	0.49		0.23 0.32 0.41

4.3. Fracture Surfaces – Qualitative observations

Figure 6 shows optical images of fracture surfaces of tablets for various combinations of initial granule SF and final tablet SF. The highest SF tablets prepared from the lowest SF granules (highest deformation potential) have the smoothest surfaces (top-left images). The smooth fracture surface suggests indiscriminate fracture of individual granules (intra-granular fracture) with minimal separation of neighboring granules (extra-granular fracture). On the other hand, the lowest SF tablets prepared from the highest SF granules (lowest deformation potential) have the roughest surfaces (bottom-right images). The presence of intact three-dimensional granule structures in the fracture surface suggests that neighboring granules were preferentially separated (extra-granular fracture).

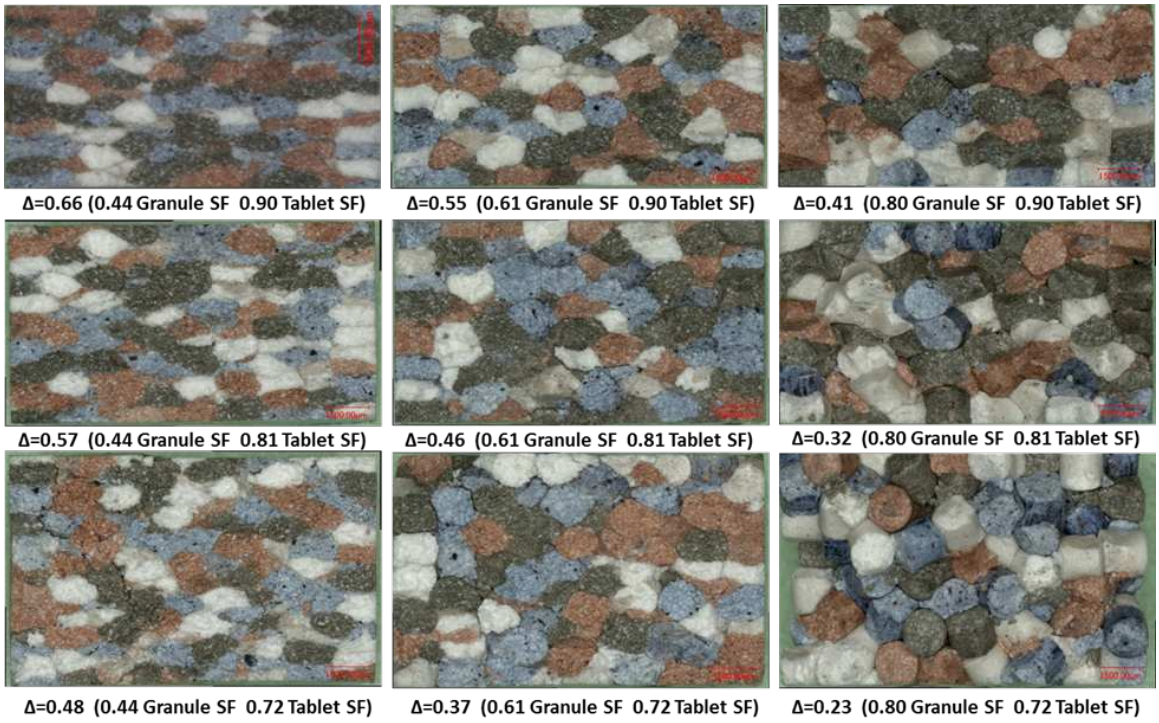

Figure 6. Optical Images of Fracture Surfaces of Tablets Produced from Colored Granule Mixtures. Granule solid fraction increases left-to-right and tablet solid fraction increases bottom-to-top.

In Figure 7, optical images of fracture surfaces of the two halves of a tablet with a high deformation potential (top image) and a tablet with a low deformation potential (bottom image) are shown. Adjacent locations of the two paired surfaces are identified by A1 and A2, B1 and B2, and so on. The smoothest fracture surfaces (top image) have greater color match between the two parts, if superimposed, compared to the roughest fracture surface (bottom image). This observation suggests that fracture of individual granules (intra-granular fracture) and/or separation of neighboring granules of the same color (extra-granular fracture) contributed to the color match between the two surfaces in the top image. Alternatively, separation of neighboring granules of different colors (extra-granular fracture) resulted in color mismatch between the two surfaces of the bottom image.

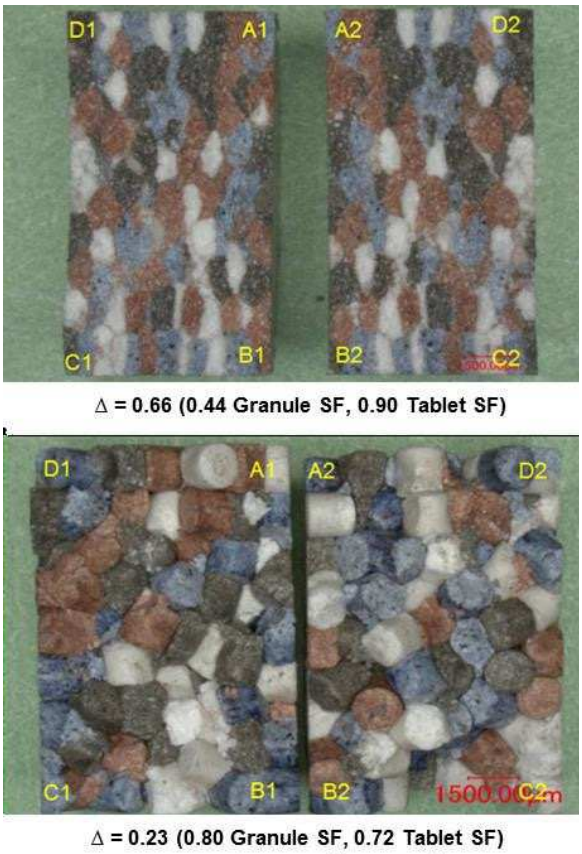

Figure 7. Optical Images of Fracture Surfaces of the Two Halves of Tablets. Top and bottom images are for the highest and lowest deformation potential, respectively.

The extent of color match and mismatch between mating fracture surfaces was qualitatively estimated using ImageJ software. Results are mapped for tablets of varying deformation potential in Figure 8. The black color denotes mating fracture surfaces where granules were the same color on both sides. Red indicates mating fracture surfaces where granule colors were mis-matched. At a given tablet SF, color match area decreases as granule SF increases (left to right). On the other hand, at a given granule SF, color match area decreases as tablet SF decreases (top to bottom). The extent of color match varies with the deformation potential. The largest color match area (black area in the top-left image) corresponds to the highest deformation potential, and vice versa (red area in the bottom-right image is the largest). This observation is consistent with the optical images presented in Figure 7.

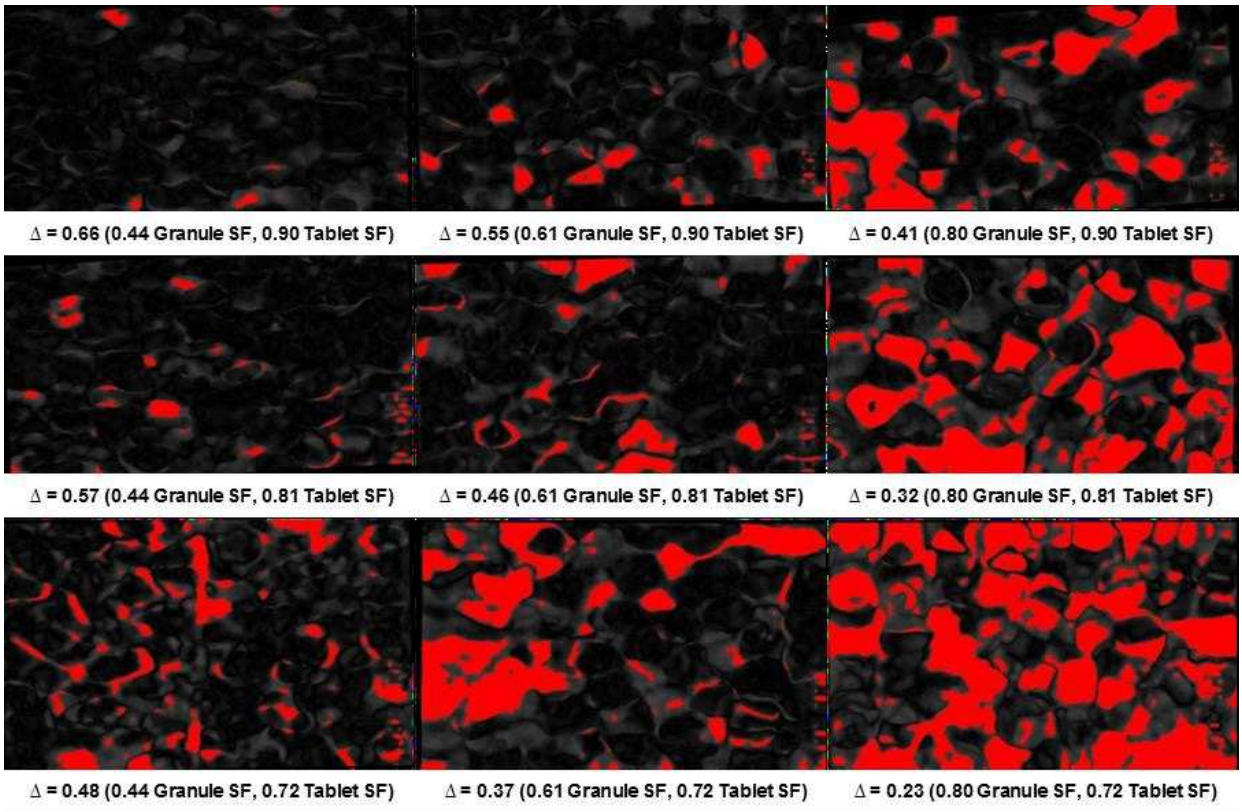

Figure 8. Color Match (Black) and Mismatch (Red) Areas Between Fracture Surfaces of the Two Halves of Tablets as a Function of Deformation Potential (Δ). Deformation potential decreases in both left-to-right and top-to-bottom directions.

4.4. Fracture Surfaces – Quantitative observations

Quantitative estimations of A_{EG} using the grid-overlay technique (Figure 4) are presented in Table 3 and are plotted in Figure 9. The figure shows proportions of intra-granular fracture areas (A_{IG}) plotted against the deformation potential (Δ). Interestingly, the A_{IG} of tablets are collapsed into a single line in this plot. Over a wide range of both initial granule SF and final tablet SF, the mode of granule fracture appears to be a function of deformation potential ***only***. A_{IG} increases linearly to approximately 100% as the deformation potential increases to a maximum value of approximately 0.66. The linear fit when extrapolated slightly, passes through an x-intercept value of approximately 0.21.

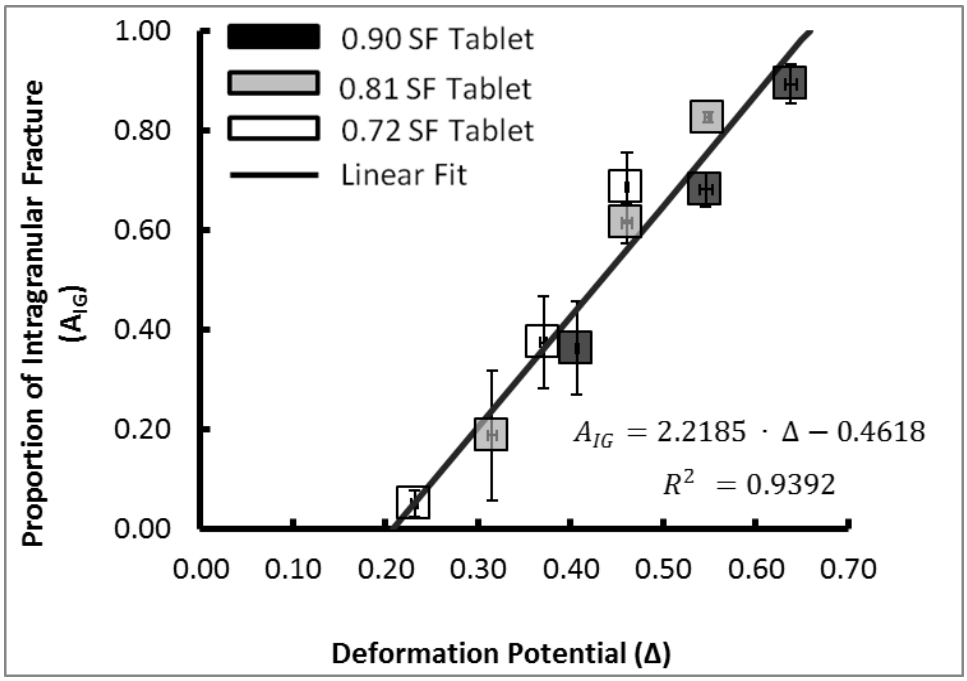

Figure 9. Proportion of Intra-granular Fracture as a Function of Deformation Potential. Open, grey and black markers represent nominally 0.72, 0.81 and 0.90 SF tablets, respectively.

This suggests that a critical deformation potential, (Δ_c) exists, below which the tablet may not have a coherent structure and would not fracture intra-granularly if the final tablet SF is not greater than the initial SF of the granule bed at least by 0.21.

4.5. Tensile Strength of Tablets

Tablet tensile strengths, σ_T, are tabulated in Table 3 and plotted as a function of the deformation potential in Figure 10. The figure shows that TS increases with deformation potential at any given tablet SF. Comparing the results in Figure 9 and Figure 10 shows that despite the comparable A_{IG} at a given deformation potential, tablets with higher SF have higher TS. This suggests that higher intra-granular strength may contribute to the higher TS of tablets even when intra-granular fracture areas are the same. The slope of the linear fit is also higher at a higher tablet SF. One should take caution in extrapolating the data as certain condition may not be physically achievable. For example, for 0.58-0.61 granule packing fraction, by definition, granule SF needs to be >1 to achieve a condition of 0.25 deformation potential in a 0.90 SF tablet, which is not physically possible. It should be noted that minor surface flattening (not more

than 5% of the tablet diameter estimated by visual observation) of the low SF tablets prepared from low SF granules was observed at the tablet/platen contacts during the breaking force test.

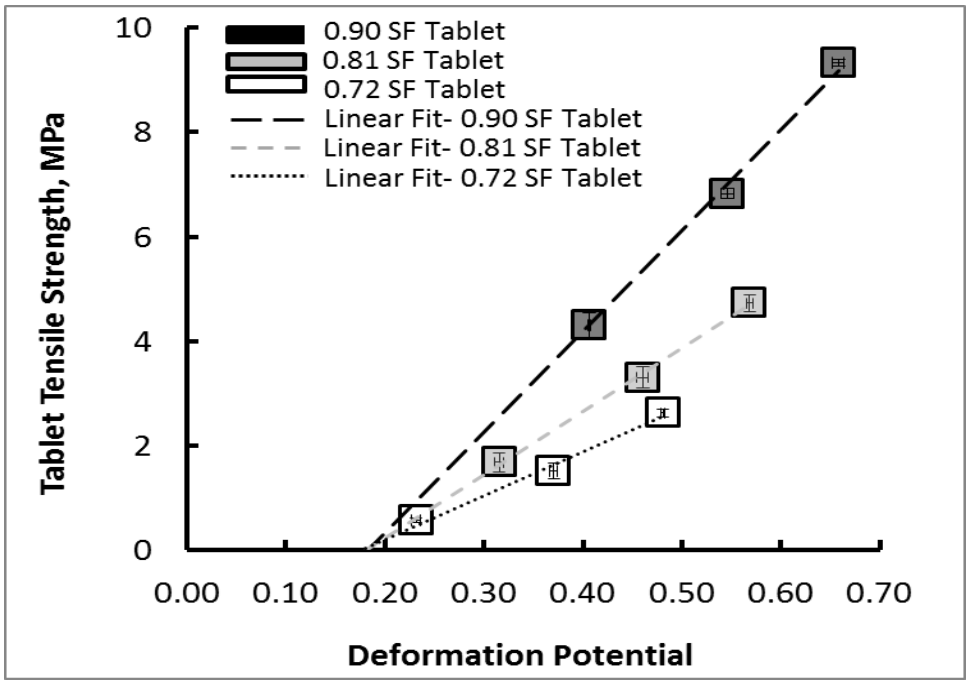

Figure 10. Tablet Tensile Strength Versus Deformation Potential. Open, grey and black markers represent nominally 0.72, 0.81 and 0.90 SF tablets, respectively. Dotted lines are the linear fits.

Interestingly, the linear fits at all tablet SF's when extrapolated, pass through a common x-intercept of ~0.18, which is close to, but smaller than, the value of 0.21 established in Figure 9. This observation suggests that between a deformation potential of 0.18 and 0.21, bonds are formed at grain boundaries. These bonds are sufficiently strong to provide measurable TS to the tablets but are not as strong as the granules. As a result, these bonds are the weakest link and fail during tablet fracture. Thus, granules separate at grain boundaries instead of cleaving. Conversely, above a deformation potential of 0.21, the bonds not only provide measurable TS to the tablets, but their strength begins to approach that of the granules. Above 0.21, a portion of the fracture surface begins to cleave the granules instead of pulling them apart.

4.6. Granule densification during tablet compression

Equation 8 was utilized to describe the densification behavior of granules as they are compressed within a tablet. Predictions of SF_G^f are tabulated in Table 3 and plotted in Figure 11. The p-values were chosen to pass through the initial conditions (square data points) and are tabulated in Table 3. For comparison in Figure 11, additional data are included from the work of Johansson et al. [20]. In Johansson's work, MCC pellets were coated with lubricant, pressed into tablets, pulled apart again, and the granule solid fractions were measured directly. The figure shows that Equation 8 provides the expected trending behavior and also describes Johansson's data nicely.

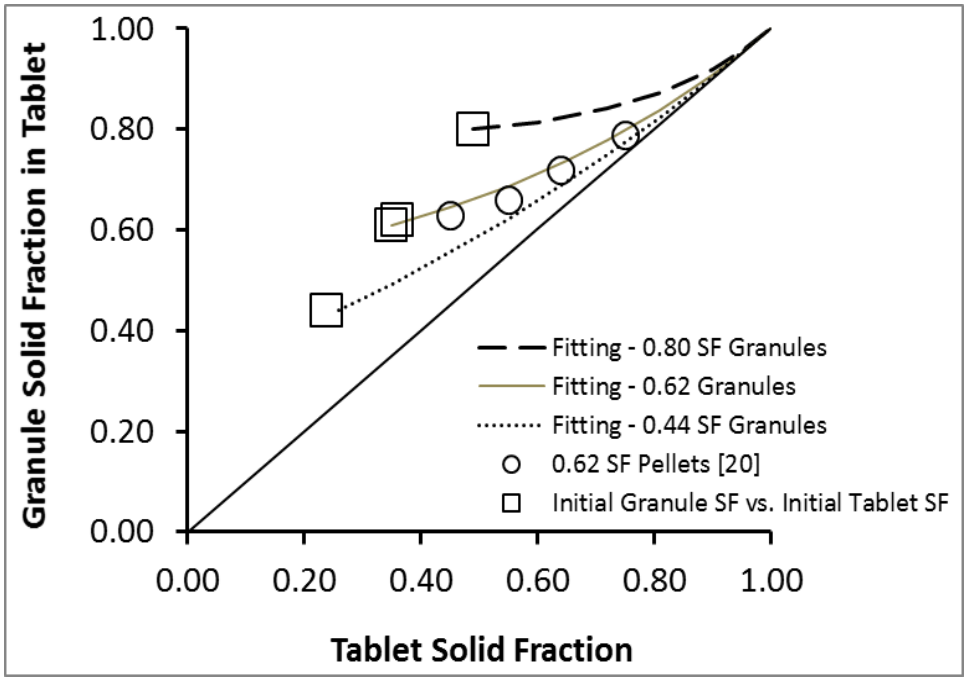

Figure 11. Exponential Fitting Curves (Dotted Lines) to Estimate Final Granule Solid Fraction in Tablets. Circle markers (O) are experimental results from literature [20].

4.7. Estimation of granule TS

Predictions of SF_G^f were used as input into Equation 7 to estimate the intra-granular tensile strength, σ_{IG}, which is also tabulated in Table 3. Estimating the granule tensile strength in this way assumes that granules which have already been compacted once maintain their strength

when re-compacted to a still-higher SF within the tablet. This turns out to be a poor assumption as discussed below.

Table 3. Quantitative Study Results

SF_G^i	SF_T	Δ *(Eq11)*	A_{IG} *(Eq 5)*	σ_T (MPa)	SF_G^f *(Eq 8)*	σ_{IG} (MPa) (Eq 7)	σ_{EG} (MPa) (Eq 1)
0.444	0.723	0.463	0.762	2.70	0.751	4.80	-4.04
0.444	0.719	0.459	0.630	2.62	0.748	4.70	-0.90
0.444	0.721	0.461	0.665	2.56	0.750	4.75	-1.78
0.608	0.719	0.369	0.472	1.61	0.777	5.73	-2.08
0.608	0.725	0.375	0.288	1.34	0.781	5.88	-0.49
0.608	0.718	0.368	0.363	1.61	0.777	5.71	-0.72
0.803	0.722	0.232	0.058	0.58	0.841	8.85	0.07
0.803	0.725	0.235	0.020	0.53	0.842	8.90	0.36
0.803	0.717	0.227	0.071	0.62	0.840	8.76	-0.01
0.444	0.812	0.552	0.814	4.90	0.825	7.94	-8.40
0.444	0.807	0.547	0.831	4.74	0.821	7.71	-9.93
0.444	0.807	0.547	0.831	4.56	0.821	7.71	-11.95
0.608	0.804	0.454	0.570	3.21	0.834	8.41	-3.68
0.608	0.814	0.464	0.622	3.18	0.841	8.83	-6.11
0.608	0.814	0.464	0.648	3.54	0.841	8.83	-6.22
0.803	0.810	0.320	0.202	1.66	0.872	10.92	-0.68
0.803	0.806	0.316	0.051	1.51	0.870	10.79	1.01
0.803	0.800	0.310	0.309	1.88	0.868	10.61	-2.02
0.444	0.895	0.635	0.937	9.24	0.899	13.12	-48.37
0.444	0.905	0.645	0.874	9.37	0.908	13.97	-22.49
0.444	0.895	0.635	0.865	9.37	0.899	13.12	-14.60
0.608	0.896	0.546	0.719	6.72	0.905	13.63	-10.94
0.608	0.903	0.553	0.673	6.89	0.911	14.18	-8.12
0.608	0.889	0.539	0.651	6.88	0.899	13.10	-4.70
0.803	0.898	0.408	0.449	4.31	0.918	14.92	-4.32
0.803	0.897	0.407	0.263	4.07	0.918	14.86	0.23
0.803	0.895	0.405	0.374	4.55	0.916	14.73	-1.54

4.8. Evaluation of Extra-granular bonding

With estimated values of A_{IG}, σ_{IG}, and σ_T, tabulated in Table 3, and given the relation $A_{EG}= 1-A_{IG}$, it was possible to calculate a numerical result for σ_{EG} that would satisfy Equation 1. These results are also tabulated in Table 3. However, many of the predictions provide a negative value, which is not physically reasonable. The negative value occurs because the estimate of σ_{IG} is too high. In fact the estimate of σ_{IG} is so high that the term $A_{IG}* \sigma_{IG}$ in Equation 1 already exceeds the measured tablet tensile strength, σ_T. Thus, the actual value of σ_{IG} is necessarily lower than that predicted by Equation 7 and plotted in Figure 5. In other words, the granule matrix becomes weaker when re-compacted within the tablet.

5. Discussion

The experimental results in this study have implications to improve the current understanding of tablet TS. In the literature, the perception is that during the diametrical breaking force test tablets prepared from granules fracture only extra-granularly (around the granules) [18, 21], and the TS of tablets is governed by the bonding force and the bonding area between the neighboring granules that are separated. This would suggest that the strength of granules in the tablet matrix would have little or no impact on the TS of tablets. However, tablet fracture surfaces were directly mapped in this study, and clearly demonstrate that tablets fracture both intra- and extra-granularly. The extent of each fracture type depends on the deformation potential *only*. This would give a new perspective understanding of the TS of tablets prepared from deformable granules and would help future development of a mechanistically based quantitative model to predict TS of tablets.

The results suggest that in contrary to the common perception, higher intra-granular strength would improve the measured TS of tablets. Therefore, materials with high compaction properties such as MCC, HPMC, etc. would be beneficial to tablet strength even when granulated. Other plastically deformable systems are also expected to fracture in the same fashion. However, a broader application of these findings for formulation development would require additional work. The coefficients in the model are formulation dependent. Therefore, the granule TS versus granule SF relation and the fracture mode of tablets need to be understood for non-plastically

deforming systems such as lactose, mannitol, or their mixtures with MCC, which would have different compaction behavior or fracture mechanics than MCC.
The mechanistic model proposed in this report predicts the intra-granular strength at the final granule solid fraction in tablets. However, the predicted intra-granular strength was higher than the experimental measured tablet tensile strength would allow, resulting in an unrealistic estimation of extra-granular bond strength. This is attributed to potential weakening of the granules due to fracture or cracking of granules, which could occur to a limited extent during the tablet compression process. In general, the exponential equation (Eq. 7, Figure 5) predicts higher intra-granular strength than what is realized in the tablets.

At a given tablet SF, smaller deformation potential produces weaker tablets. The SF and TS of granules are higher if produced using higher compaction pressure. Irrespective of the granules SF, the same amount of compression pressure is required to achieve the final tablet SF. However, high SF granules produce tablet matrices that are not homogeneous, have larger extra-granular pores. The deformation potential for this system is low, and the tablet exhibits lower strength in a diametrical breaking force test. With that respect, the results would supplement the UCC (unified compaction curve) model from the material attribute perspectives. According to the UCC model, the TS of tablets formed from plastically deformable dry granules is lower if the difference between the cumulative compression pressure (granulation plus tableting) and the granulation pressure the materials experience is smaller, and vice versa [34].

6. Conclusions

The use of monodisperse colored granule mixtures in this study enabled us to visualize the fate of granules during the confined compression process. Granules in the die cavity, even at low SF, tended to maintain their integrity where they underwent plastic deformation with associated change in shape and increase in SF under compressive pressure. Low SF granules deformed extensively and neighboring granules surfaces intermingled more than high SF granules and produce more homogeneous tablet matrices. At a high deformation potential, tablets fractured mostly intra-granularly (cleavage of individual granules). In contrast, at a low deformation potential, tablets preferentially fractured extra-granularly. Quantification of these fracture types demonstrated that the proportion of intra-granular fracture was a linear function of the

deformation potential. The granule bed needs to exceed the critical deformation potential to obtain a coherent tablet. The TS of tablets increased nearly linearly with the deformation potential with higher slope of the latter relationship at higher tablet SF. Tablet tensile strength was modeled as a function of the intra-granular strength at final solid fraction in tablets weighted by the proportion of intra-granular fracture of tablets. However, the results indicated that the intra-granular bond strength is reduced by an unknown extent, preventing an accurate assessment of both intra-granular and extra-granular bond strength.

Acknowledgement

The authors would like to thank Jeff Hanson of Eli Lilly and Company for assistance with the image analysis using ImageJ software.

References

[1] Brick RM, Pense AW, Gordon RB. 1977. Structure and Properties of Engineering Materials. In McGraw-Hill Series in Materials Science and Engineering. New York: Mcgraw-Hill college, 4^{th} Ed.

[2] Barret C, Tetelman A, Nix W. 1973. The Principles of Engineering Materials, Prentice Hall Englewood Cliffs, New Jersey.

[3] Kendall K, Howard A, Birchall J. 1983. The relation between porosity, microstructure and strength, and the approach to advanced cement-based materials. Philosophical Transaction of the Royal Society of London A130: 139-153.

[4] Kendall K. 1988. Agglomerate strength. Powder Metallurgy 31: 28-31.

[5] Launey M, Ritchie R. 2009. On the fracture toughness of advanced materials. Advanced Materials 21: 2103-2110.

[6] Sun CC, Himmelspach M. 2006. Reduced tabletability of roll compacted granules as a result of granule size enlargement. J Pharm Sci 59: 200-206.

[7] Herting M, Kleinebudde P. 2008. Studies on the reduction of tensile strength of tablets after roll compaction/dry granulation. Eur J Pharm Biopharm 70: 372-379.

[8] Patel S, Dahiya S, Sun CC, Bansal A. 2011. Understanding size enlargement and hardening of granules on tabletability of unlubricated granules prepared by dry granulation. J Pharm Sci 100: 758-766.

[9] He X, Secreast P, Amidon G. 2007. Mechanistic study of the effect of roller compaction and lubricant on tablet mechanical strength. J Pharm Sci 96: 1342-1355.

[10] Roberts R, Rowe R and York P. 1995. The relationship between the fracture properties, tensile strength and critical stress intensity factor of organic solids and their molecular structure. Int J Pharm 125: 157-162.

[11] Al-Nasassrah M, Podczeck F, Newton J. 1998. The effect on an increase chain length on the mechanical properties of polyethylene glycols. Eur J Pharm Biopharm 46: 31-38.

[12] York P, Bassam F, Rowe R, Roberts R. 1990. Fracture mechanics of microcrystalline cellulose powders. Int J Pharm 66: 143-148.

[13] Farkas D. 2000. Atomistic studies of intrinsic crack-tip plasticity, MRS Bulletin, 25: 35-38.

[14] Sun CC, 2011. Decoding Powder Tabletability: Roles of Particle Adhesion and Plasticity. J Adhesion Sci Technol, 25: 483-499.

[15] Rumpf H. 1962. The strength of granules and agglomerates. In Knepper WA, editor. Agglomeration, New York: Interscience p 379-418

[16] Nystrom C, Alderborn G, Duberg M, Karehill P. 1993. Bonding surface area and bonding mechanism-two important factors for the understanding of powder compactibility. Drug Dev Ind Pharm 19: 2143–2196.

[17] Adolfsson A, Gustafsson C, Nystrom C. 1999. Use of tablet tensile strength adjusted for surface area and mean interparticulate distance to evaluate dominating bonding mechanisms. Drug Dev Ind Pharm 25: 753–764.

[18] Johansson B, Wikberg M, Ek R, Alderborn G. 1995. Compression behavior and compactibility of microcrystalline cellulose pellets in relationship to their pore structure and mechanical properties. Int J Pharm 117: 57-73.

[19] Johansson B, Alderborn G. 1996. Degree of pellet deformation during compaction and its relationship to the tensile strength of tablets formed of microcrystalline cellulose pellets. Int J Pharm 132: 207-220.

[20] Johansson B, Nicklasson F, Alderborn G. 1998. Effect of pellet size on degree of deformation and densification during compression and on compactability of microcrystalline cellulose pellets. Int J Pharm 163: 35-48.

[21] Alderborn G. 2013. Particle, Tablets and Compaction. In Aulton M, Taylor K, editors. Aulton's Pharmaceutics: The Design and Manufacture of Medicines, 4th ed., London: Elsevier Ltd. p 534.

[22] Mitra B, Hilden J, Litster J. 2015. Novel use of monodisperse granules to deconvolute impacts of granule size versus granule solid fraction on tablet tensile strength, Adv Powder Technol 26: 553-562.

[23] Sun CC. 2008. Mechanism of moisture induced variations in true density and compaction properties of microcrystalline cellulose. Int J Pharm 346: 93-101.

[24] Bultmann. 2002. Multiple compaction of microcrystalline cellulose in a roller compactor. Eur J Pharm Biopharm 54: 59-64.

[25] Hilden J, Earle G. 2011. Prediction of roll compacted ribbon solid fraction for quality by design development. Powder Technology 213: 1–13.

[26] Francke J, Lammens R, Steffens K. 2006. A uniform method to describe the mechanical strength of round flat and convex-faced tablets. In 5th World Meeting on Pharmaceutics, Biopharmaceutics and Pharmaceutical Technology, Geneva, Switzerland.

[27] Hilden J, Polizzi M, Zettler A. 2017. Note on the Use of Diametrical Compression to Determine Tablet Tensile Strength. J Pharm Sci 106: 418-421

[28] http://fiji.sc/Fiji

[29] http://rsb.info.nih.gov/ij/

[30] Schneider C, Rasband S, Eliceiri W. 2012. NIH Image to ImageJ: 25 years of image analysis. Nature Methods 9: 671-675.

[31] Thevenaz P, Ruttimann U, Unser M. 1998. A pyramid approach to subpixel registration based on intensity. Image Processing, IEEE Transactions 7: 27-41.

[32] Ryshkewitch E. 1953. Compression strength of porous sintered alumina and Zirconia. J Amer Ceramic Soc 36: 65-68.

[33] Scott GD, Kilgour DM. 1969. The density of random close packing of spheres. British J Applied Physics 2: 863.

[34] Farber L, Hapgood KP, Michaels JN, Fu X-Y, Meyer R, Johnson M-A, Li F. 2008. Unified compaction curve model for tensile strength of tablets made by roller compaction and direct compression. Int J Pharm 346: 17-24

Figure Caption

Figure 1. Illustration of the Approach to Quantify Intra-granular and Extra-granular Fracture of Tablets.

Figure 2. Illustration of Deformation of Granules During Compression.

Figure 3. Schematic Diagram of the Study Design.

Figure 4. Image Analysis Using a Grid Overlay.

Figure 5. Tensile Strength of Granules Versus Granule Solid Fraction.

Figure 6. Optical Images of Fracture Surfaces of Tablets Produced from Colored Granule Mixtures. Granule solid fraction increases left-to-right and tablet solid fraction increases bottom-to-top.

Figure 7. Optical Images of Fracture Surfaces of the Two Halves of Tablets. Top and bottom images are for the highest and lowest deformation potential, respectively.

Figure 8. Color Match (Black) and Mismatch (Red) Areas Between Fracture Surfaces of the Two Halves of Tablets as a Function of Deformation Potential (Δ). Deformation potential decreases in both left-to-right and top-to-bottom directions.

Figure 9. Proportion of Intra-granular Fracture as a Function of Deformation Potential. Open, grey and black markers represent nominally 0.72, 0.81 and 0.90 SF tablets, respectively.

Figure 10. Tablet Tensile Strength Versus Deformation Potential. Open, grey and black markers represent nominally 0.72, 0.81 and 0.90 SF tablets, respectively. Dotted lines are the linear fits.

Figure 11. Exponential Fitting Curves (Dotted Lines) to Estimate Final Granule Solid Fraction in Tablets. Circle markers (O) are experimental results from literature [20].